The effect of the Coriolis force on Faraday waves

By Gour Chandra Mondal[1] and Krishna Kumar[2]

[1]*Physics and Applied Mathematics Unit, Indian Statistical Institute, 203 Barrackpore Trunk Road, Kolkata 700108, India*

[2]*Department of Physics and Meteorology, Indian Institute of Technology, Kharagpur 721302, India* (kumar@phy.iitkgp.ernet.in)

Linear stability of the free surface of a thin sheet of a viscous fluid on a vertically vibrated rigid plate, in the presence of a uniform and slow rigid body rotation about the vertical axis, is presented. The Coriolis force delays the onset of parametrically excited surface waves. The creation of Faraday waves is always possible by raising the acceleration amplitude above a critical value, if the angular frequency ω_v of the vertical vibration is much larger than four times the angular velocity $\boldsymbol{\omega}_r$ of the rotating plate. The surface waves may be harmonic or superharmonic with the imposed vibration in a thin sheet of slowly rotating viscous fluids at small vibration frequencies. This leads to the possibility of a tri-critical point at the onset of the surface instability in thin layers of a viscous fluid. Subharmonic, harmonic and superharmonic waves with different wavenumbers may coexist at the instability onset in the presence of a small Coriolis force, which is a qualitatively new result.

Keywords: Faraday waves; Coriolis force; tri-critical point

1. Introduction

Faraday waves (Faraday 1831) appear on the free surface of a horizontal fluid layer by subjecting the latter to a sinusoidal forcing in vertical plane. These are parametrically forced standing waves on the free surface. These waves oscillate subharmonically with the external vibration. They are excited as the forcing amplitude is raised above a critical value (Benjamin & Ursell 1954; Miles & Henderson 1990; Kumar 1996; Miles 1999; Perlin & Schultz 2000). Experiments (see, for instance, Douady 1990; Ciliberto *et al*. 1991; Fauve *et al*. 1992; Edwards & Fauve 1994; Bechhoefer *et al*. 1995; Kumar & Bajaj 1995; Binks & van de Water 1997; Kudrolli *et al*. 1998; Raynal *et al*. 1999) in the last decade have shown a variety of interesting patterns in the Faraday set-up. The forced surface waves could also be synchronous (Kumar 1996; Müller *et al*. 1997; Cerda & Tirapegui 1997) with the external forcing in the presence of large dissipation. This usually occurs in thin layers of viscous fluids at low forcing frequencies. This leads to the possibility of a bi-critical point at the instability onset, where both subharmonic and harmonic (synchronous) surface waves can be excited for the same value of forcing amplitude a. Although multi-critical points, where many different solutions coexist at a given point in the parameter space, occur in many systems in condensed matter physics (for a recent review, see Aharony 2002), electrical circuits (Kuznetsov *et al*. 1996; Berthet *et al*. 2002) and hydrodynamical

systems (e.g. Becerril & Swift 1997; Ahlers & Bajaj 1999; Zhang & Gubbins 2000), etc., they are rarely observed in experiments at the onset of primary instability. The nonlinear process of pattern selection in the vicinity of a multi-critical point in fluids may lead to superlattice patterns (see, for example, Rogers *et al.* 2000) due to the availability of several critical modes with different wavenumbers and frequencies. On the other hand, the waves in rotating fluids are known to lead to interesting phenomena and mathematical problems (see, for example, Chandrasekhar 1961; Greenspan 1968; Barcilon 1968; Franklin 1972; Witham 1974; Whitehead *et al.* 1990; Hu *et al.* 1997; Kumar *et al.* 2002). The Coriolis force breaks the mirror symmetry of the convective flow patterns (Veronis 1957) and introduces competition between two sets of rolls at an angle of *ca.* 60° to each other in the Rayleigh–Bénard set-up (Küppers & Lortz 1969; Donnelly 1986). The effect of Coriolis force on the onset of Faraday waves is yet to be investigated.

In this paper, we present the study of Faraday waves in a thin sheet of a viscous fluid subjected to a uniform and slow rotation about the vertical axis. The rotation imposes a body force (Coriolis force), which breaks the mirror symmetry of the flow due to parametrically excited surface waves. In addition, this provides a rare physical system to investigate the role of Coriolis force on a multi-critical point, which may be accessible at the instability onset. The Coriolis force delays the Faraday waves on the free surface. However, the Faraday (subharmonic) waves can always be excited at the onset of surface instability if the angular frequency $\omega_{\rm v}$ of the vertical vibration is much greater than four times the angular frequency $\omega_{\rm r}$ of rigid-body motion of the fluid. The surface waves may also be synchronous with the vertical vibration in a thin sheet of viscous fluid. In addition, we observe interesting instability phenomena in a thin layer of a slowly rotating viscous fluid (whose viscosity is approximately 10 times the viscosity of water). Firstly, the synchronous surface waves develop an additional local maxima, when a is raised above certain value. Any point on the free surface moves up and attains two different local maxima in one period of external forcing. The wavenumber of these waves is double that of the synchronous waves. Superharmonic waves at the instability onset are possible in parametrically forced viscous fluids. Secondly, different responses (e.g. subharmonic, harmonic and superharmonic) with different wavenumbers may coexist for the same forcing amplitude. This leads to the interesting possibility of a tri-critical point as the primary instability, which is rare in any physical system. We believe that the results presented here are verifiable experimentally.

2. Hydrodynamic system

We consider a thin layer (of thickness h) of an incompressible fluid with uniform density ρ and kinematic viscosity ν, resting on a horizontal plate that is subjected to a vertical simusoidal oscillation of amplitude a and angular frequency $\omega_{\rm v}$. The whole system is rotating slowly with a uniform angular velocity $\omega_{\rm r}$ about the vertical axis. The basic state of rest in a frame fixed with the rigid horizontal plate has the time-dependent pressure field

$$P(t) = P_{\rm air} - \rho g(t) z - \tfrac{1}{2}\rho|\boldsymbol{\omega}_{\rm r} \times \boldsymbol{x}|^2,$$

where $\boldsymbol{x}$ stands for the position vector in the horizontal plane from the axis of rotation and $\boldsymbol{\omega}_{\rm r} = (0, 0, \omega_{\rm r})$. In experiments, the side walls will create a pressure

gradient to compensate for the effects of centrifugal force at least for small rotation rates. The concavity of the free surface is also small, if the centrifugal force is much smaller than the gravitational force. This may be achieved in a circular container of diameter 20 cm rotating slowly (*ca.* 2–16 RPM) about the vertical axis passing through its centre. The angle

$$\theta = \arctan\left(\frac{\omega_r^2 r}{g}\right)$$

between the vertical and the surface normal near the edge of the circular container is very small (up to 0.036 rad). These constraints idealize the physical situation but allow us to investigate the role of the Coriolis force on the Faraday waves. This approach is similar to that used by Chandrasekhar (1961, § 95) to study the effect of rotation on the Rayleigh–Taylor instability at the interface of two immiscible ideal (zero viscosity) fluids. Under these constraints, the free surface is assumed to be initially flat, stationary and located at $z = 0$. The oscillation is equivalent to a temporally modulated gravitational acceleration, $g(t) = g - a\cos(\omega_v t)$. Linearizing about the basic state, the dimensionless perturbation equations for relevant fields then read

$$\partial_t \boldsymbol{v} = -\nabla p + \nabla^2 \boldsymbol{v} - \tau(\boldsymbol{e}_3 \times \boldsymbol{v}), \tag{2.1}$$

$$\nabla \cdot \boldsymbol{v} = 0, \tag{2.2}$$

where $\boldsymbol{v}(x, y, z, t) \equiv (u, v, w)$ is the velocity field, $\boldsymbol{e}_3$ is a unit vector in the vertically upward direction, p is the pressure field, and $\tau = 2\omega_r h^2/\nu$ is the dimensionless rotation rate. In the above, length-scales are made dimensionless by the thickness h of the fluid layer, time by the viscous time-scale h^2/ν, the fluid velocity field by ν/h, the pressure field by $\rho\nu^2/h^2$ and the rotation rate by ν/h^2. Taking the curl of the momentum equation (2.1) twice, we obtain the following equations for the vertical vorticity Z and the vertical velocity w, respectively:

$$(\partial_t - \nabla^2) Z = \tau \partial_z w, \tag{2.3}$$

$$(\partial_t - \nabla^2)\nabla^2 w = -\tau \partial_z Z. \tag{2.4}$$

As the fluid rests on a rigid plate, all three velocity components must vanish on the plate. These conditions may be translated as

$$w = \partial_z w = Z = 0 \quad \text{at } z = -1. \tag{2.5}$$

As soon as the instability sets in, the free surface is destabilized. It is then located at $z = \zeta(\boldsymbol{x}, t)$, where $\boldsymbol{x} = (x, y)$, and it obeys the kinematic boundary condition (Lamb 1932, § 9) given by

$$\partial_t \zeta = w|_{z=\zeta}. \tag{2.6}$$

Other boundary conditions can be obtained by considering the stress tensor at the free surface, given by

$$\Pi_{jk} = -p\delta_{jk} + (\partial_j v_k + \partial_k v_j) + \mathcal{G}(t)\zeta\delta_{jk}, \tag{2.7}$$

The last term above is the stress due to surface deformation in the effective gravitational acceleration $\mathcal{G}(t) = G - A\cos(\Omega t)$. The parameters $G = gh^3/\nu^2$, $A = ah^3/\nu^2$,

and $\Omega = \omega_v h^2/\nu$ are, respectively, the Galileo number, the dimensionless form of forcing amplitude and the dimensionless vibration frequency. As there are no tangential stress components at the free surface, for the linear problem we have $\Pi_{xz} = \Pi_{yz} = 0$ at $z = \zeta$. Since the tangential stress vanishes everywhere at the free surface, we may also write $\partial_x \Pi_{xz} = \partial_y \Pi_{yz} = 0$ at $z = \zeta$, which may further be reduced by using the equation of continuity (2.2) to

$$(\nabla_{\mathrm{H}}^2 - \partial_{zz}) w|_{z=\zeta} = 0, \tag{2.8}$$

where $\nabla_{\mathrm{H}}^2 = \partial_{xx} + \partial_{yy}$ is the horizontal Laplacian. The normal component of the stress tensor at the free surface must be equated to the surface tension σ times the curvature of the free surface, which for the dimensionless linear problem reads

$$\Pi_{zz}|_{z=\zeta} = \mathcal{C}^{-1} \nabla_{\mathrm{H}}^2 \zeta, \tag{2.9}$$

where $\mathcal{C} = \rho\nu^2/\sigma h$ is the capillary number. Equations (2.7) and (2.9) lead to the expression for the pressure at the free surface,

$$p|_{z=\zeta} = 2(\partial_z w)|_{z=\zeta} + \mathcal{G}(t)\zeta - \mathcal{C}^{-1} \nabla_{\mathrm{H}}^2 \zeta. \tag{2.10}$$

Taking horizontal divergence of equation (2.1) we get an expression,

$$\nabla_{\mathrm{H}}^2 p = (\partial_t - \nabla^2)\partial_z w + \tau Z, \tag{2.11}$$

for the pressure everywhere in the fluid. Elimination of the pressure field p from equations (2.9)–(2.11) leads to the following condition at the free surface:

$$(\partial_t - \nabla^2)\partial_z w|_{z=\zeta} = 2\nabla_{\mathrm{H}}^2 (\partial_z w)|_{z=\zeta} + \mathcal{G}(t)\nabla_{\mathrm{H}}^2 \zeta - \mathcal{C}^{-1} \nabla_{\mathrm{H}}^4 \zeta - \tau Z. \tag{2.12}$$

The fields are expressed in the normal modes of the horizontal plane, i.e. $\sin(\boldsymbol{k} \cdot \boldsymbol{x})$, where the horizontal wavenumber ($k^2 = k_x^2 + k_y^2$) can take any real and positive value. We now replace $w(\boldsymbol{x}, z, t)$ by $w(z, t)\sin(\boldsymbol{k} \cdot \boldsymbol{x})$, $\zeta(\boldsymbol{x}, t)$ by $\zeta(t)\sin(\boldsymbol{k} \cdot \boldsymbol{x})$, and the differential operator ∇_{H}^2 by $-k^2$. For a consistent linear stability, we compute all the fields at the free surface by Taylor expanding them about $z = 0$ plane, and keeping only the linear terms. The relevant equations then read

$$[\partial_t - (\partial_{zz} - k^2)](\partial_{zz} - k^2) w = -\tau \partial_z Z, \tag{2.13}$$

$$[\partial_t - (\partial_{zz} - k^2)] Z = \tau \partial_z w, \tag{2.14}$$

$$w = \partial_z w = Z = 0 \quad \text{at } z = -1, \tag{2.15}$$

$$w|_{z=0} = \partial_t \zeta, \tag{2.16}$$

$$(\partial_{zz} + k^2) w = \partial_z Z = 0 \quad \text{at } z = 0, \tag{2.17}$$

$$[(\partial_t - \partial_{zz} + 3k^2)\partial_z w + \tau Z]|_{z=0} = -[G - A\cos(\Omega t) + \mathcal{C}^{-1} k^2] k^2 \zeta. \tag{2.18}$$

The set of equations (2.13)–(2.18) constitutes the complete linear stability problem for a laterally unbounded layer of rotating viscous fluid, under parametric oscillation. The linear stability problem may also be written in terms of vertical velocity w and the surface deformation ζ by eliminating the vertical vorticity Z and transforming boundary conditions on the vertical vorticity in terms of the vertical velocity.

3. Stability analysis

The stability of the system (2.13)–(2.18) is analysed by applying Floquet theory (Kumar & Tuckerman 1994). The surface deformation $\zeta(t)$ and the vertical velocity $w(z,t)$ are expressed as

$$\zeta(t) = \mathrm{e}^{\mu t} \sum_{n=-\infty}^{\infty} \zeta_n \mathrm{e}^{\mathrm{i}n\Omega t}, \tag{3.1}$$

$$w(z,t) = \mathrm{e}^{\mu t} \sum_{n=-\infty}^{\infty} w_n(z) \mathrm{e}^{\mathrm{i}n\Omega t}. \tag{3.2}$$

The Floquet exponent μ can be expressed as $\mu = s + \mathrm{i}\alpha\Omega$, where s and α can take any real and finite value. The solutions corresponding to $\alpha = 0$ and $\alpha = \frac{1}{2}$ are referred to as harmonic and subharmonic solutions, respectively. We arrive, with these substitutions, at the following sixth-order differential equation for w_n,

$$[(D^2 - k^2)\{(D^2 - \beta_n^2)^2 + \tau^2 D^2\}]w_n = 0, \tag{3.3}$$

with the boundary conditions

$$w_n|_{z=-1} = 0, \tag{3.4}$$

$$Dw_n|_{z=-1} = 0, \tag{3.5}$$

$$(D^2 - k^2)(D^2 - \beta_n^2)Dw_n|_{z=-1} = 0, \tag{3.6}$$

$$[s + \mathrm{i}(\alpha + n)\Omega]\zeta_n = w_n|_{z=0}, \tag{3.7}$$

$$(D^2 + k^2)w_n|_{z=0} = 0, \tag{3.8}$$

$$(D^2 - k^2)(D^2 - \beta_n^2)w_n|_{z=0} = 0, \tag{3.9}$$

$$\left[D^3 - \frac{1}{\beta_n^2}(D^2 - k^2)(D^2 - \beta_n^2) - \left(\gamma_n^2 + \frac{\tau^2}{\beta_n^2}\right)D\right]w_n = [G - A\cos(\Omega t) + k^2\mathcal{C}^{-1}]k^2\zeta_n \quad \text{at } z = 0, \tag{3.10}$$

where $\beta_n^2 = k^2 + [s + \mathrm{i}(\alpha + n)\Omega]$, $\gamma_n^2 = \beta_n^2 + 2k^2$ and $D \equiv \mathrm{d}/\mathrm{d}z$. As we are interested in stability boundaries and critical values of the forcing amplitude A and the wavenumber k, we set $s = 0$ in the above system of equations. The general solution of equation (3.3) then reads

$$w_n(z) = A_n \cosh q_1 z + B_n \cosh q_2 z + C_n \cosh q_3 z + D_n \sinh q_1 z + E_n \sinh q_2 z + F_n \sinh q_3 z, \tag{3.11}$$

where $q_i \equiv q_i(n)$ $(i = 1, 2, 3)$ for each n are roots of the cubic equation

$$q^3 - 2\mathrm{i}(\alpha + n)\Omega q^2 + [\tau^2 - (\alpha + n)^2\Omega^2]q + \tau^2 k^2 = 0. \tag{3.12}$$

The application of conditions (3.4)–(3.9) to the general solution (3.11) leads to a matrix equation for every n

$$\mathcal{B}(n)\boldsymbol{\Psi}(n) = \boldsymbol{\Phi}(n), \tag{3.13}$$

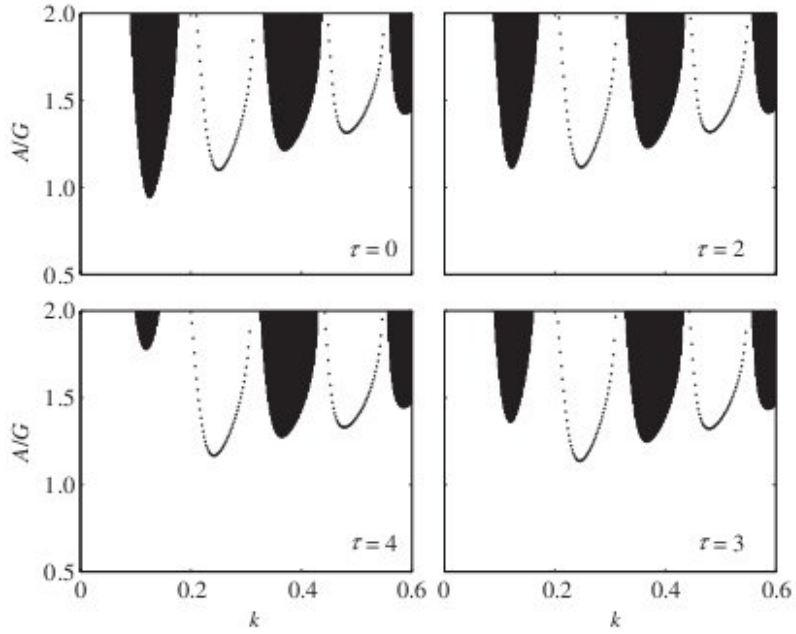

Figure 1. Stability diagrams for four different values of the rotation parameter τ. The fluid parameters chosen are relevant for a water–glycerol mixture ($\nu \approx 0.1\,\mathrm{cm^2\,s^{-1}}$). Other parameters are $G = 2.7 \times 10^3$, $\mathcal{C} = 4.7 \times 10^{-4}$ and $\Omega = 11$. The zones bounded by dots and the shaded zones are for $\alpha = 0$ and $\alpha = 0.5$, respectively.

where $\mathcal{B}(n)$ is a 6×6 matrix. The transpose of the column matrix $\boldsymbol{\Psi}(n)$ is

$$\boldsymbol{\Psi}^{\mathrm{T}}(n) = (A_n, B_n, C_n, D_n, E_n, F_n).$$

Similarly, the transpose of $\boldsymbol{\Phi}(n)$ is

$$\boldsymbol{\Phi}^{\mathrm{T}}(n) = (0, 0, 0, \mathrm{i}\{\alpha + n\}\Omega\zeta_n, 0, 0).$$

The operation by $\mathcal{B}^{-1}$ on the matrix equation (3.13) converts six unknowns A_n, B_n, C_n, D_n, E_n and F_n in terms of one unknown ζ_n. The application of the normal stress condition (3.10) at the free surface then leads to the recursion relation

$$\mathcal{Q}_n\zeta_n = A(\zeta_{n-1} + \zeta_{n+1}), \tag{3.14}$$

where $\mathcal{Q}_n$ for each n is known. The kinematic condition (3.7) gives $w_0(z = 0) = 0$ for $[s + \mathrm{i}(\alpha + n)] = 0$. This, together with boundary and continuity conditions, ensures that $w_0(z) = 0$ for all possible values of z. Therefore, for the case of harmonic response ($\alpha = 0$),

$$\mathcal{Q}_0^h = \frac{2}{k}(Gk + \mathcal{C}^{-1}k^3).$$

The recursion relation (3.14) is equivalent to a generalized eigenvalue problem (Kumar & Tuckerman 1994)

$$\mathcal{Q}\boldsymbol{X} = A\mathcal{D}\boldsymbol{X}, \tag{3.15}$$

where $\mathcal{Q}$ is a diagonal square matrix with complex elements $\mathcal{Q}_n$. The matrix $\mathcal{D}$ is such that $\mathcal{D}_{j+1,l} = 1$ and $\mathcal{D}_{j,l+1} = 1$. All other elements of the banded matrix $\mathcal{D}$

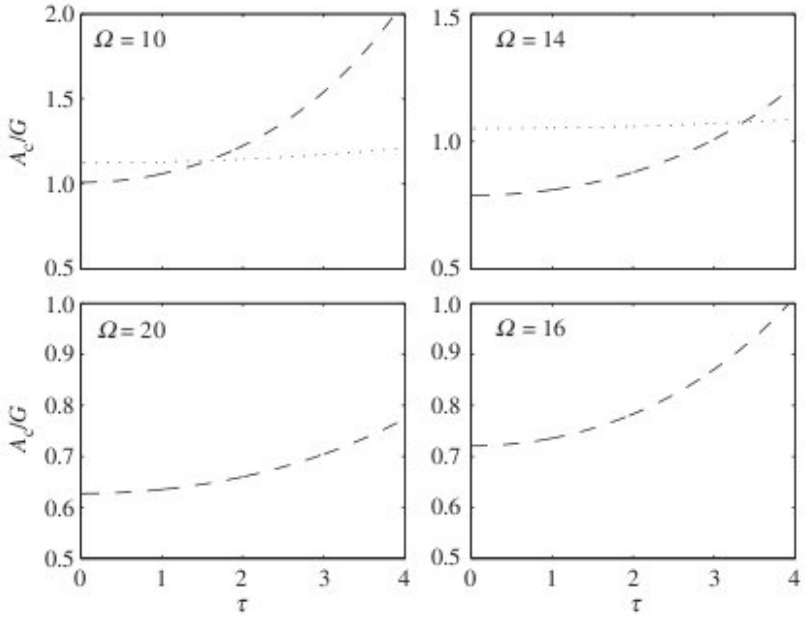

Figure 2. Minima of the reduced acceleration amplitude (A_c/G) for the lowest two tongues (top) and the lowest tongue (bottom) as a function of rotation parameter τ for different values of the dimensionless vibration frequency Ω. Plots are arranged by increasing values of Ω. The dashed and dotted curves show the minima of the first subharmonic and the first harmonic tongues, respectively. The bi-critical points shown are relevant for water–glycerol mixture. Other parameters are $G = 2.7 \times 10^3$ and $\mathcal{C} = 4.7 \times 10^{-4}$.

are identically zero. The column matrix $\boldsymbol{X}$ consists of ζ_n. An ordinary eigenvalue problem can also be written from (3.15) as

$$(\mathcal{Q}^{-1}\mathcal{D})\boldsymbol{X} = \frac{1}{A}\boldsymbol{X}. \tag{3.16}$$

The real eigenvalues of $\mathcal{Q}^{-1}\mathcal{D}$ are the inverse of the forcing amplitude A. The eigenvalues are determined numerically with a pre-assigned accuracy. The plot of real positive values of A with respect to k gives the marginal stability curve as the growth rate $s(A, k) = 0$. By choosing $\alpha = 0$ and $\alpha = \frac{1}{2}$, stability zones for harmonic and subharmonic solutions are determined. They are usually in the form of tongues (see figure 1). The minimum of the lowest tongue gives critical value of the forcing amplitude A_c and the critical wavenumber k_c. For computation of A_c, the Floquet series (3.1), (3.2) is truncated to some finite value. All the computations are done here with truncation to 21 for subharmonic and 22 for harmonic solutions, although the results converge for more than 10 terms of the series. We have computed test cases taking 100 terms of the expansion, and we found no change in the results.

4. Subharmonic and harmonic surface waves

Figure 1 shows the effect of Coriolis force on the stability zones of the parametrically excited waves. The regions outside the tongue-like zones correspond to a stable and flat free surface. Inside these regions, the free surface is unstable to any perturbations.

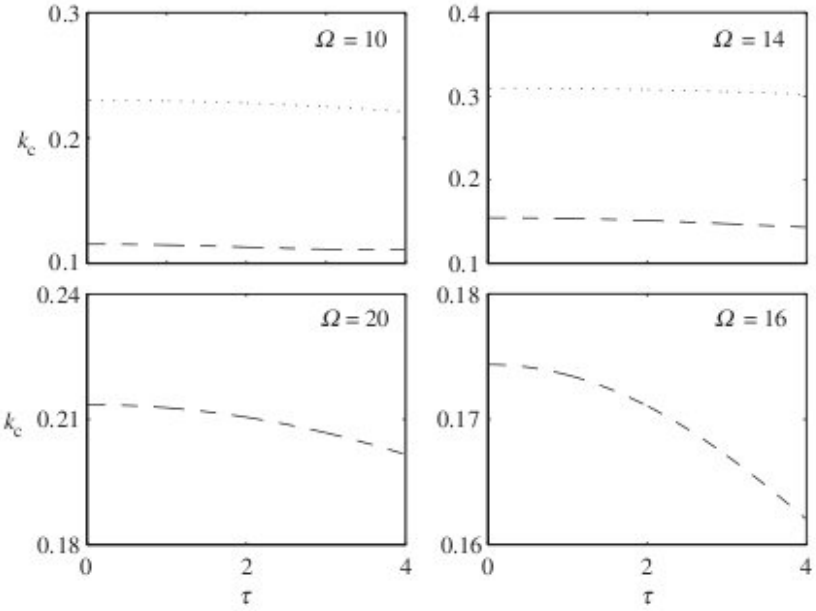

Figure 3. Critical wavenumbers k_c corresponding to the lowest points of the first two tongues (top) and the lowest tongue (bottom) as a function of τ. All fluid parameters and symbols are as in figure 2.

On the boundaries separating stable from unstable zones, the growth rates of all perturbations are exactly zero. The possible frequencies of the growing standing waves inside the shaded zones can only be odd multiples of $\Omega/2$. The standing waves for parameters inside the zones marked by dots can have only those frequencies which are integer multiples of Ω. Two sets of the possible response of the flat surface under parametric excitation are mutually exclusive. Therefore, the two types of zones never intersect each other. The four graphs, clockwise from the top left, are arranged by increasing rotation rate τ. The first tongue, corresponding to a subharmonic response with respect to vertical vibration, moves up faster in the A–k-plane, while other tongues move up very slowly (see figure 2). Consequently, the onset of Faraday waves is delayed. In the presence of Coriolis force, all the tongues also move leftward to lower wavenumbers (figure 3). The second tongue, which corresponds to harmonic surface waves, becomes the lowest tongue with increasing τ (lower row of figure 1). This signifies a bifurcation from subharmonic to synchronous surface waves. Just before this bifurcation, the system goes through a bi-critical point (upper right, figure 1). In the absence of rotation, this behaviour is possible only in highly viscous fluids (Kumar 1996). However, rotation can force synchronous surface waves even in less viscous fluids like water at low frequencies.

The minima of the reduced forcing amplitude (A_c/G) for the first two lowest tongues are plotted in figure 2 for different values of the forcing frequency Ω. The dashed curves correspond to the subharmonic response and dotted curves to synchronous waves. For $\Omega \gg 2\tau$ (i.e. $\omega_v \gg 4\omega_r$), Faraday waves can always be excited on the flat surface of a rotating viscous fluid sheet by raising the forcing amplitude A above a critical value A_c. The value of A_c increases with rotation rate. This is because the rotation generates vertical vorticity. This increases dissipation in the

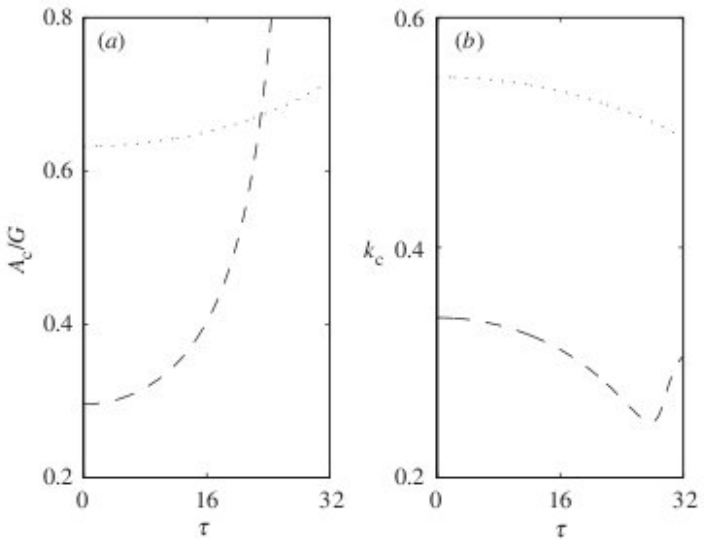

Figure 4. Critical values of (a) the reduced acceleration (A_c/G) and (b) critical wavenumbers k_c for the lowest two tongues as a function of rotation parameter τ. The dashed and dotted curves are for subharmonic and harmonic waves, respectively. Other parameters are relevant for water: $G = 2.7 \times 10^5$, $\mathcal{C} = 5 \times 10^{-6}$ and $\Omega = 60$.

Table 1. *Range of physical parameters used for computation*

liquid	ρ (g cm^{-3})	σ (dyn cm^{-1})	ν (cm^2 s^{-1})	h (mm)	$\omega_v/2\pi$ (Hz)	figure no.
water–glycerol	1.0–1.1	60–75	0.1	2.0–3.0	1–4	1–3, 5
water	1.0	70.0	0.01	2.5–3.0	1–4	4

system, making the threshold of surface waves higher. For smaller values of Ω, the surface waves may be synchronous with vertical vibration. The dependence of the wavenumbers, corresponding to the minima of the first two tongues, as a function of τ is shown in figure 3. The critical wavenumber k_c decrease slowly with increasing rotation rate for a fixed value of vibration frequency. This happens until $\tau \lesssim \Omega/2$. For $\tau \gg \Omega/2$, the critical wavenumber increase with rotation rate (see figure 4). The slow decrease in wavenumber with increasing rotation rate for smaller values of τ may be due to competition among various dissipative mechanisms. Once the instability sets in, the Coriolis force is available to enlarge the cells of fluid motion overcoming the resistance from the rigid plate. With decreasing wavenumber, the resistance of the bottom slowly increases and ultimately prevents any further wavenumber decrease.

Figure 4 shows the possibility of harmonic waves in a thin layer of water rotating slowly (*ca.* 13 RPM). The lowest wavenumber corresponding to the subharmonic response shows a dip with increasing τ. But the amplitude of the harmonic response becomes smaller than that for the subharmonic response. The Coriolis force may lead to the possibility of harmonic waves even in low-viscosity fluid such as water. Table 1 lists the range of physical parameters for which the computations are carried out.

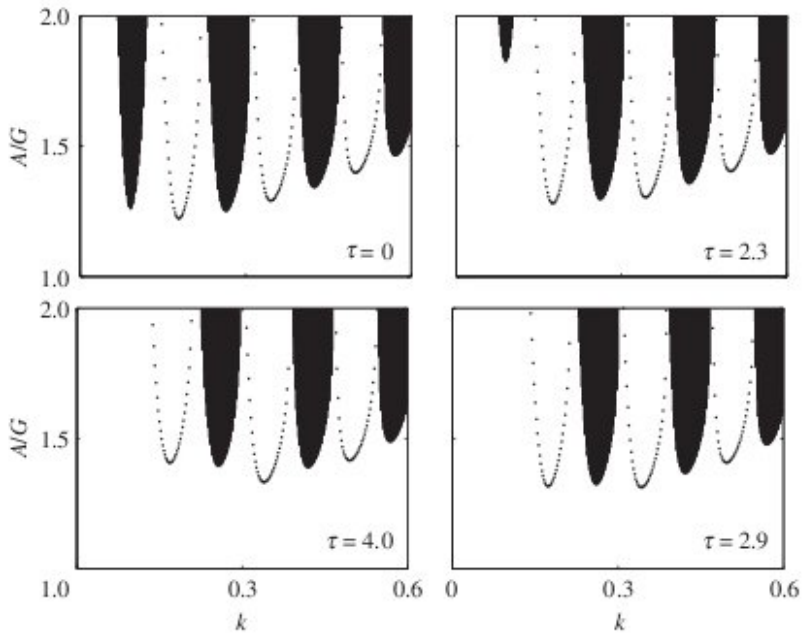

Figure 5. Stability zones showing a tri-critical point and superharmonic waves in viscous sheet of water–glycerol mixture ($G = 2.7 \times 10^3$, $\mathcal{C} = 4.7 \times 10^{-4}$ and $\Omega = 7.5$). The shaded zones and zones bounded by dots are for $\alpha = 1/2$ and $\alpha = 0$, respectively. With increasing τ (clockwise from top left), harmonic response goes to a tri-critical point for $\tau = 2.9$, where surface waves with wavenumbers k_1, $1.5k_1$ and $2k_1$ with k_1 the wavenumber of the first harmonic response coexist at the instability onset. Further increase in τ leads to superharmonic waves as primary instability.

5. Tri-critical point and superharmonic waves

Figure 5 shows the stability diagram for a thin sheet of water–glycerol mixture ($\nu \approx 0.1$ cm^2 s^{-1}, thickness $h \approx 3$ mm) at dimensionless vibration frequency $\Omega = 7.5$ (1–2 Hz) for different rotation rates. The fluid parameters are chosen such that the surface waves are synchronous (Kumar 1996; Müller *et al.* 1997; Cerda & Tirapegui 1997) with vibration frequency in the absence of rotation. In the presence of even small rotations, all tongues are shifted upwards. The first subharmonic tongue is pushed up quicker than the others, as the waves with largest wavelength (the smallest k_c) face maximum resistance from the rigid bottom in a thin sheet of viscous fluid. Other tongues move up slowly and at different rates. This leads to the interesting possibility of observing a tri-critical point in a Faraday experiment with very slow rotation ($\tau \approx 3$, i.e. for 4–5 RPM). The surface waves with three different wavenumbers k_1, $1.5k_1$ and $2k_1$, where k_1 is critical wavenumber of first harmonic tongue, coexist at the same forcing amplitude at the onset of surface instability in the case of a tri-critical point. A slight increase in rotation rate ($\tau = 4$, i.e. *ca.* 6 RPM) leads to the possibility of superharmonic surface waves with critical wavenumber $k_2 = 2k_1$ at the instability onset, even at very slow rotation.

Figure 6 shows the time dependence of the critical mode corresponding to the lowest points of various tongues of figure 5 and compares them with the sinusoidal forcing. All the curves in this figure are plotted over twice the time period of vibration

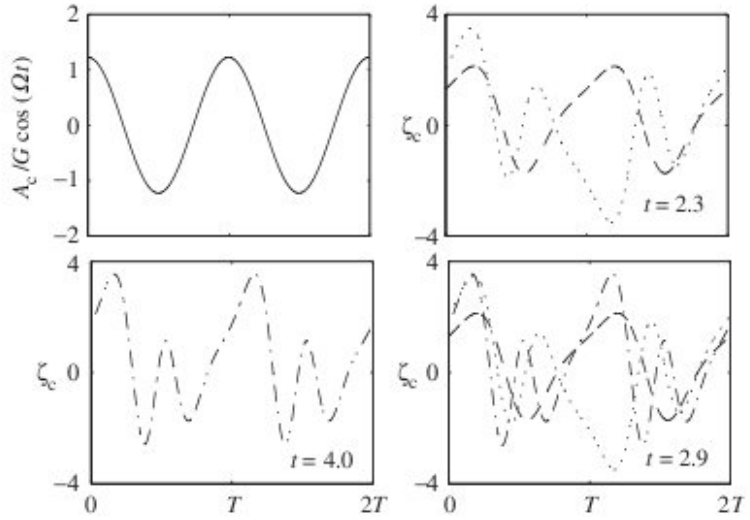

Figure 6. Time dependence of the critical modes for the first harmonic (dashed curves), the second subharmonic (dotted curves) and the superharmonic (dashed dotted curves) surface waves for increasing values of rotation rate τ. The top left shows the forcing for a comparison of the critical modes with vertical vibration over a period twice the period T $(= 2\pi/\Omega)$. All parameters are same as in figure 5.

T (where $T = 2\pi/\Omega$). Although the forcing in the vertical direction is sinusoidal, the response at the free surface is periodic but quite distorted. The critical mode (dashed curve) for $\tau = 2.3$ is synchronous with the external vibration and corresponds to the lowest point of the harmonic curve of figure 5 for the same value of τ. The dotted curve corresponds to the lowest point of the second subharmonic tongue, for the same value of τ. That is why it shows three peaks over a period of $2T$.

All three responses occur at the same value of the forcing amplitude A_c for $\tau = 2.9$. This leads to an interesting possibility of a tri-critical point at the instability onset in Faraday experiment. Further increases in τ lead to superharmonic waves at the instability onset (lower left). The critical mode shows two peaks over one period of vibration. The fluid surface at a given point is raised twice by the time one vibration is completed.

6. Conclusions

We have presented the stability analysis of the free surface of a viscous fluid under vertical vibration and subjected it to a uniform slow rotation about the vertical axis. The subharmonic waves are suppressed at relatively higher rotation rates. Synchronous and superharmonic waves could be excited on the free surface of a thin sheet of viscous fluid, due to Coriolis force. Superharmonic waves are likely for $4\omega_r \gg \omega_v$. For viscous fluids such as water–glycerol mixtures or silicon oil, these effects may be observed at small rotation rate (a few revolutions per minute). The results predict a new tri-critical point where surface waves with response wavenumbers k_c, $1.5k_c$ and $2k_c$ could be simultaneously forced at the instability onset. Superharmonic solu-tions and the tri-critical point at the onset of primary instability in a parametrically

excited sheet of fluid may be possible at low rotation rates. These results may have interesting consequences in pattern selection in parametrically forced systems.

This work is sponsored partly by the Department of Science and Technology (DST), Government of India, through its grants under the project 'Pattern-forming instabilities and interface waves', and partly by the Sponsored Research and Industrial Consultancy (SRIC) unit of the Indian Institute of Technology, Kharagpur, India. We benefited from fruitful discussions with Professor G. P. Sastry.

References

Aharony, A. 2002 Preprint, cond-mat/0201576.

Ahlers, G. & Bajaj, K. M. S. 1999 In *Proc. IMA Workshop on Pattern Formation in Continuous and Coupled Systems* (ed. M. Golubitsky, D. Luss & S. Strogatz). Springer.

Barcilon, V. 1968 *Mathematika* **15**, 93.

Becerril, R. & Swift, J. B. 1997 *Phys. Rev.* E **55**, 6270.

Bechhoefer, J., Ego, V., Manneville, S. & Johnson, B. 1995 *J. Fluid Mech.* **288**, 325.

Benjamin, T. B. & Ursell, F. 1954 *Proc. R. Soc. Lond.* A **225**, 505.

Berthet, R., Petrosyan, A. & Roman, B. 2002 *Am. J. Phys.* **70**, 744.

Binks, D. & van de Water, W. 1997 *Phys. Rev. Lett.* **78**, 4043.

Cerda, E. & Tirapegui, E. 1997 *Phys. Rev. Lett.* **78**, 859.

Chandrasekhar, S. 1961 *Hydrodynamic and hydromagnetic stability.* Oxford: Clarendon.

Ciliberto, S., Douady, S. & Fauve, S. 1991 *Europhys. Lett.* **15**, 23.

Donnelly, R. J. 1986 *Phys. Rev. Lett.* **57**, 2524.

Douady, S. 1990 *J. Fluid Mech.* **221**, 383.

Edwards, W. S. & Fauve, S. 1994 *J. Fluid Mech.* **278**, 123.

Faraday, M. 1831 *Phil. Trans. R. Soc. Lond.* A **52**, 319.

Fauve, S., Kumar, K., Laroche, C., Beysens, D. & Garrabos, Y. 1992 *Phys. Rev. Lett.* **68**, 3160.

Franklin, J. N. 1972 *J. Math. Analysis Applic.* **39**, 742.

Greenspan, H. P. 1968 *The theory of rotating fluids.* Cambridge University Press.

Hu, Y., Ecke, R. E. & Ahlers, G. 1997 *Phys. Rev.* E **55**, 6928.

Kudrolli, A., Pier, B. & Gollub, J. P. 1998 *Physica* D **123**, 99.

Kumar, K. 1996 *Proc. R. Soc. Lond.* A **452**, 1113.

Kumar, K. & Bajaj, K. M. S. 1995 *Phys. Rev.* E **52**, R4606.

Kumar, K. & Tuckerman, L. S. 1994 *J. Fluid Mech.* **279**, 49.

Kumar, K., Chaudhuri, S. & Das, A. 2002 *Phys. Rev.* E **65**, 026311.

Küppers, G. & Lortz, D. 1969 *J. Fluid Mech.* **35**, 609.

Kuznetsov, A. P., Kuznetsov, S. P., Sataev, I. R. & Chua, L. O. 1996 *Int. J. Bifurcat. Chaos* **6**, 119.

Lamb, H. 1932 *Hydrodynamics.* Cambridge University Press.

Miles, J. 1999 *J. Fluid Mech.* **395**, 321.

Miles, J. W. & Henderson, D. 1990 *A. Rev. Fluid Mech.* **22**, 143.

Müller, H. W., Wittmer, H., Wagner, C., Albers, J. & Knorr, K. 1997 *Phys. Rev. Lett.* **78**, 2357.

Perlin, M. & Schultz, W. W. 2000 *A. Rev. Fluid Mech.* **32**, 241.

Raynal, F., Kumar, S. & Fauve, S. 1999 *Eur. Phys. J.* B **9**, 175.

Rogers, J. L., Schatz, M. F., Brausch, O. & Pesch, W. 2000 *Phys. Rev. Lett.* **85**, 4281.

Veronis, G. 1957 *J. Fluid Mech.* **5**, 401.

Whitehead, J. A., Stern, M. E., Flierl, G. R. & Klinger, B. A. 1990 *J. Geophys. Res.* **95**, 9585.

Witham, G. B. 1974 *Linear and nonlinear waves.* New York: Interscience.

Zhang, K. & Gubbins, D. 2000 *Phil. Trans. R. Soc. Lond.* A **358**, 899.